Transverse acoustic spin and torque from pure spinning of objects

M. Farhat [1] P.-Y. Chen,[2] M. Amin,[3] A. Alù,[4,5] and Y. Wu[1,*]

[1]*Computer, Electrical, and Mathematical Science and Engineering (CEMSE) Division, King Abdullah University of Science and Technology (KAUST), Thuwal 23955-6900, Saudi Arabia*
[2]*Department of Electrical and Computer Engineering, University of Illinois at Chicago, Chicago, Illinois 60607, USA*
[3]*College of Engineering, Taibah University, Madinah 42353, Saudi Arabia*
[4]*Photonics Initiative, Advanced Science Research Center, City University of New York, New York, New York 10031, USA*
[5]*Physics Program, Graduate Center, City University of New York, New York, New York 10016, USA*

Acoustic spin has been recently explored for many applications. In particular, transverse acoustic spin was demonstrated for inhomogeneous acoustic fields. In this Letter, we show the emergence of acoustic spin and torque in rotating acoustic objects of the same physical properties as the surrounding, to single out the effects purely due to rotation. The spinning of a cylindrical column of air or water in the same medium possesses intrinsic spin angular momentum, and we study the torque and force it experiences in evanescent acoustic fields. The resulting discontinuity can thus scatter sound in unusual ways, including a negative radiation force, although it has no imaginary part in its parameters.

Objects that experience moving and/or spinning motion undergo intrinsically distinct scattering signatures [1–8] and require special treatment different from the one of objects at rest [9–20]. For example, it was shown in Ref. [21] that a body rotating around its axis of symmetry in a QED vacuum spontaneously emits energy. A simple cylindrical inhomogeneity with finite (or infinite) conductivity is also shown to possess a different scattering response that may be solved by means of the instantaneous rest-frame technique [22,23]. Several promising applications were proposed with spinning building blocks, e.g., waveguide rotation sensor systems [8] or gyroscopes [24,25]. In the same vein, Censor *et al.* analyzed the governing equations of pressure waves (acoustics) [26] in moving or rotating media, and showed that an equivalent wave equation may be derived [27]. The same analysis was extended to elastic waves in solids [28,29]. More recently, this formalism was used to investigate the possibility of a scattering cancellation technique for spinning cylindrical acoustic objects [30] or analyzing [31,32] metamaterials with spinning components [33].

In a different context, Anhäuser *et al.* proposed quantitatively the transfer of acoustic orbital angular momentum to an absorbing millimeter-sized object, that resulted in making it spin [34]. Then, Bliokh *et al.* analyzed in detail the inherent analogies between acoustic waves and electromagnetic waves [35] and showed that despite the apparent scalar nature of acoustic waves [36], several vectorial effects, such as spin [37,38] and orbital angular momentum [39] can take place in both frameworks. More recently, Meng *et al.* used an active acoustic particle that experiences a negative radiation force (i.e., acoustic pulling) when excited by a single acoustic wave [40].

In this Letter we investigate the interaction of a spinning acoustic volume with an incident acoustic plane wave in terms of torque, radiation, and scattering forces. We treat the scattering object by its acoustic polarizabilities in a semianalytical way. We show that although it has no imaginary part in its parameters, it can lead to torque and acoustic force. What is striking is that it is possible to obtain positive and negative radiation force. This shows its potential application in the domain of acoustic pulling, which was previously achieved in a different way [40] with either the active particle (nonzero imaginary part of the density) or the composite incident signal (two plane waves with directions making a finite angle). Our proposal lifts these constraints and may represent a rather easier way to implement these intriguing effects. Our work thus considers a different avenue, that relies on the object instead of the external source. Moreover, with this concept we can obtain both acoustic torque and acoustic pulling force, with the same design and by only using incident plane waves.

Consider a medium that is uniformly rotating [with the rotation axis coinciding with $\hat{\mathbf{e}}_z$, as schematized in Fig. 1(a)] at angular velocity Ω. We formulate a coupled system, with details shown in the Supplemental Material (SM) [41], leading to the following wave equation (modified Helmholtz equation),

$$\frac{\partial^2 p}{\partial r^2} + \frac{1}{r}\frac{\partial p}{\partial r} + \left(k_n^2 - \frac{n^2}{r^2}\right)p = 0, \tag{1}$$

with the modified wave number

$$k_n = \frac{i}{c}\sqrt{4\Omega^2 + \gamma_n^2}, \tag{2}$$

*ying.wu@kaust.edu.sa
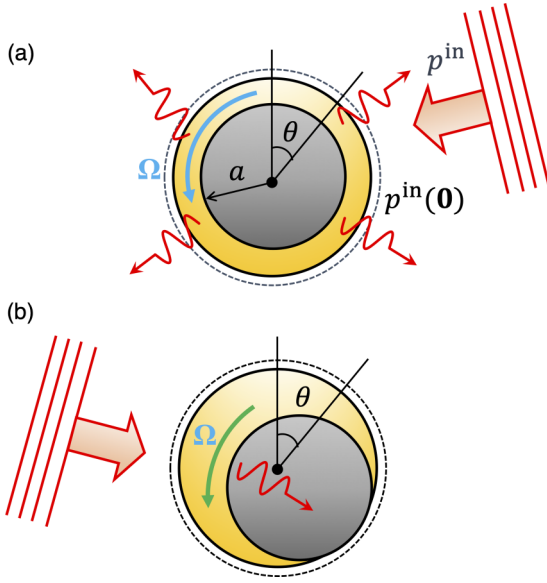
FIG. 1. (a) Schematic view (x-y plane) of the single cylindrical scattering particle of radius a (in gray color) lying inside a homogeneous infinitely extended medium (here air, in yellow color, with the dashed circle meaning the domain extends to infinity) and the incident plane wave excitation impinging on it. The acoustic monopole scattering is due to pure spinning, resulting from expansion and compression of the object. (b) Schematic representation of the acoustic dipole scattering, resulting in oscillatory linear motion of the object. The scales of motion in this figure are exaggerated, as in reality the motion or expansion of the particle are only perturbations.

with $\gamma_n = i(n\Omega - \omega)$ the rotation Doppler-shifted frequency (see SM [41]). Equation (1) is actually a Helmholtz-like equation, expressed in polar coordinates, with the effective (spinning) wave number k_n. When there is no spinning (i.e., $\Omega = 0$), we can see from Eq. (2) that we recover $k = \omega/c$. The behavior of k_n, i.e., the spinning wave number, can be found in

Ref. [30]. As the parameter γ_n is complex number, k_n has both propagating (real part) and damped (imaginary part) components. Similar to the case at rest, the governing equation has to be complemented by appropriate continuity conditions at the physical interfaces of the problem [26]. For spinning media, the continuity conditions must take into account the relative movement. It can be shown that p should remain continuous as before; however, the continuity of $1/(\rho \partial_r p)$ should be replaced by the continuity of the normal displacement

$$\zeta_r = \frac{\gamma_n v_r + \Omega v_\theta}{\gamma_n^2 + \Omega^2} = \frac{(2\Omega^2 - \gamma_n^2)\partial_r p - 3i\gamma_n \Omega n p/r}{\rho(4\Omega^2 + \gamma_n^2)(\Omega^2 + \gamma_n^2)}. \quad (3)$$

By inspection of Eq. (3), again by letting $\Omega = 0$, we get the usual continuity as acoustics at rest.

We consider the scattering problem of a spinning cylinder of radius a under the excitation of a plane and monochromatic acoustic wave. As illustrated in Fig. 1(a), the cylinder's axis of rotation is its axis of symmetry which is along the $\hat{\mathbf{e}}_z$ direction. The expansion of the fields and the derivation of the scattering cross section are derived in the SM [41].

By applying the continuity of p and ζ_r on the boundary $r = a$, we can show that each scattering order is given by

$$\varsigma_n = \begin{vmatrix} J_n(k_n a) & J_n(k_0 a) \\ \Pi_{J_n} & \frac{\beta_0}{k_0} J_n'(k_0 a) \end{vmatrix} \begin{vmatrix} J_n(k_n a) & -H_n^{(1)}(k_0 a) \\ \Pi_{J_n} & -\frac{\beta_0}{k_0} H_n^{(1)'}(k_0 a) \end{vmatrix}^{-1}, \quad (4)$$

where $|M|$ denotes the determinant of a matrix M and with the coefficient Π_{J_n} expressed as

$$\Pi_{J_n} = \frac{(2\Omega^2 - \gamma_n^2)k_n J_n'(k_n a) - \frac{3\gamma_n \Omega i n}{a} J_n(k_n a)}{\rho(4\Omega^2 + \gamma_n^2)(\Omega^2 + \gamma_n^2)}. \quad (5)$$

Let us first assume that $\rho = \rho_0$ and $\beta = \beta_0$, to filter out the scattering due to the inhomogeneities (i.e., $\rho/\rho_0 \neq 1$ and/or $\beta/\beta_0 \neq 1$). Further, when $k_0 a \ll 1$ and $k_n a \ll 1$, i.e., for acoustically small scatterers, we may derive the expressions of ς_n in a closed-form up to the order 4 in $\tilde{\kappa} = k_0 a$ (to simplify the notations), i.e.,

$$\varsigma_0 = i\frac{3\pi}{4}\frac{\alpha^2}{1-\alpha^2}\tilde{\kappa}^2 - i\frac{\pi\alpha^2}{32(1-\alpha^2)^2}[13 + 36\alpha^2 \log(\tilde{\kappa}/2) - \alpha^2(5 - 36\gamma_E + 8\alpha^2 + i18\pi)](\tilde{\kappa})^4 + O(\tilde{\kappa}^5),$$

(6)

$$\varsigma_{\pm 1} = i\frac{\pi}{4}\frac{\alpha}{\pm 2 + \alpha}\tilde{\kappa}^2 \pm i\frac{\pi\alpha}{32(2 \pm \alpha)^2(1 \mp 2\alpha)}\{-4 \pm \alpha[19 \mp i2\pi(\mp 1 + 2\alpha) \pm 4\gamma_E(\mp 1 + 2\alpha) + 2\alpha$$
$$\times (\pm 13 + 6\alpha \mp 4\log 2) + 4\log 2] + 4\alpha(\mp 1 + 2\alpha)\log\tilde{\kappa}\}\tilde{\kappa}^4 + O(\tilde{\kappa}^5),$$

(7)

where $\alpha = \Omega/\omega$ is the rotation ratio of the spinning object and γ_E is the Euler-Mascheroni constant. The symbol $O(\cdot)$ represents a function of the same order as $(\cdot)$ (i.e., Landau symbol) [42]. The $+$, $-$ signs in Eq. (7) correspond to the coefficient ς_1 and ς_{-1}, respectively. Here, have to emphasize that if $\alpha \to 0$, all the scattering coefficients ς_n ($\forall n \in \mathbb{Z}$) converge to zero, as we have assumed here $\rho = \rho_0$ and $\beta = \beta_0$.

The acoustic monopole scatters a pressure field given by [17]

$$p^{(m)} = -\frac{k_0 c_0}{4}\rho_0 M H_0^{(1)}(k_0 r), \quad (8)$$

with M the monopole strength [43] shown in Fig. 1(a). On the other hand, the acoustic dipole scatters a pressure field given by

$$p^{(d)} = -i\frac{k_0^2 c_0}{4}\rho_0(D_x \cos\theta + D_y \sin\theta)H_1^{(1)}(k_0 r), \quad (9)$$

with $D_{x,y}$ the dipole terms in the x, y directions, respectively. For instance, $D_x \cos\theta + D_y \sin\theta$ just corresponds to D_r, as $p^{(d)} \propto \mathbf{D} \cdot \nabla[H_0^{(1)}(k_0 r)]$ [44]. The expressions given in Eqs. (8) and (9) are reminiscent of those of the Mie development of Eq. (8) in the SM [41], i.e., the term of order $n = 0$ that is $p_0\varsigma_0 H_0^{(1)}(k_0 r)$ and $n = \pm 1$, i.e., $p_0 i(\varsigma_1 e^{i\theta} + \varsigma_{-1}e^{-i\theta})H_1^{(1)}(k_0 r)$. Here, the monopole and dipole strength can be related to the monopole and dipole acoustic polarizabilities [45], using these relations,

$$M = -i\omega\beta_0\alpha_m p_0, \quad D^{x,y} = -i\beta_0 c_0\alpha_d^{x,y}p_0. \quad (10)$$

The monopole can be expressed as $M = -4p_0\varsigma_0/(k_0 c_0\rho_0)$, whereas the dipole strengths are

$$D^x = \frac{-4}{k_0^2\rho_0 c_0}(\varsigma_1 + \varsigma_{-1})p_0, \quad (11)$$

and

$$D^y = \frac{-4i}{k_0^2\rho_0 c_0}(\varsigma_1 - \varsigma_{-1})p_0. \quad (12)$$

By combining Eqs. (8)–(12) we can derive the expressions of the different polarizabilities, i.e.,

$$\alpha_m = \frac{-4i}{k_0^2}\varsigma_0, \quad (13)$$

$$\alpha_d^x = \frac{-4i}{k_0^2}(\varsigma_1 + \varsigma_{-1}) \quad \text{and} \quad \alpha_d^y = \frac{4}{k_0^2}(\varsigma_1 - \varsigma_{-1}). \quad (14)$$

It can be seen from Eqs. (13) and (14) that the polarizabilities have the unit of a surface, as can be anticipated, in this two-dimensional (2D) scenario. These equations were derived for the most general scenario, i.e., without restrictions on the direction of the incident velocity. In order to have an effect due only to spinning, let us consider an incident velocity in the y direction. For instance, when $\Omega = 0$ and $\rho/\rho_0 \neq 1$ or $\beta/\beta_0 \neq 1$, we have $\varsigma_n = \varsigma_{-n}$, so $\alpha_d^y = 0$ and $\alpha_d^x = -i\frac{8}{k_0^2}\varsigma_1$. But, when $\Omega \neq 0$ and even if $\rho/\rho_0 = 1$ and/or $\beta/\beta_0 = 1$, we have $\alpha_d^x\alpha_d^y \neq 0$, as $\varsigma_1 \neq \varsigma_{-1}$, and as can be seen from Eq. (7). By following a particle in the co-spinning frame of reference $\mathcal{R}'$, i.e., a frame that is rotating with a frequency Ω equal to that of the fluid, it can be easily seen why $\varsigma_{-n} \neq \varsigma_n$, as these multipoles correspond to an angle $-\theta$ and θ, respectively. When there is no rotation, there is an invariance with respect to θ so both coefficients are equal. By inducing rotation, this symmetry is broken and thus the invariance is no longer valid.

Now, using Eqs. (13) and (6), we can obtain the analytical expressions ($k_0 a \ll 1$) of $\text{Im}(\alpha_m)$ and $\text{Re}(\alpha_m)$, where we assume here no material inhomogeneity, so $k_0 = k$, that is

$$\text{Re}(\alpha_m) = \frac{3\pi\alpha^2}{1 - \alpha^2}a^2 - \frac{\pi\alpha^2}{8(1 - \alpha^2)^2}f_1(ka)k^2a^4 + O[(ka)^3],$$

$$\text{Im}(\alpha_m) = \frac{9\pi^2\alpha^4}{4(1 - \alpha^2)^2}k^2a^4 + O[(ka)^3], \quad (15)$$

with $f_1(ka) = [13 - 8\alpha^4 + \alpha^2(36\gamma_E - 5) + 36\alpha^2 \log(\frac{ka}{2})]$. Similarly, using Eqs. (14) and (7), we can derive the dipole

acoustic polarizability in the quasistatic limit,

$$\text{Re}(\alpha_d^y) = \frac{2\pi^2\alpha^3}{(4 - \alpha^2)^2}k^2a^4 + O[(ka)^3],$$

$$\text{Im}(\alpha_d^y) = \frac{4\pi\alpha}{4 - \alpha^2}a^2 + \frac{2\pi\alpha f_2(ka)}{(4 - \alpha^2)^2(1 - 4\alpha^2)}k^2a^4 + O[(ka)^3], \quad (16)$$

where

$$f_2(ka) = -3\alpha^6 + 4\alpha^4\left[2\gamma_E + 3 + 2\log\left(\frac{ka}{2}\right)\right]$$
$$+ 13\alpha^2\left[13 - \gamma_E - \frac{2}{13}\log\left(\frac{ka}{2}\right)\right] + 2.$$

The real and imaginary parts of α_m and α_d^y are given in Fig. 2. Two scenarios are considered: First, we choose parameters such that the quasistatic approximation applies, that is, $ka \ll 1$, $a = 1$ m, and $\Omega/(2\pi) = 10$ Hz. This scenario is plotted in Fig. 2(a), and we can see an excellent agreement between the numerical results [Eq. (4)] and those obtained analytically [Eqs. (15) and (16)]. The resonant polarizabilities (α_m and α_d^y) correspond to the poles, that can be seen in Eqs. (15) and (16). The other scenario does not obey the quasistatic approximation, and the parameters are hence $a = 10$ m and $\Omega/(2\pi) = 100$ Hz. In this case, the polarizabilities undergo several oscillations reminiscent of Mie scattering. Here, we do not see any marked resonant effect, as before.

In this study, we are interested in investigating both torque and scattering force from spinning acoustic particles, so we consider an inhomogeneous acoustic field in order to induce transverse spin, that is, an evanescent acoustic field [37,38], with its pressure and velocity expressed as

$$p = p_0 e^{-\kappa x + ik_y y}, \quad \mathbf{v} = \frac{p_0}{\rho\omega}(i\kappa, k_y, 0)^T e^{-\kappa x + ik_y y}, \quad (17)$$

with $(\cdot)^T$ the transverse of a given matrix. The spin of this inhomogeneous (evanescent) field can be shown to be $\mathbf{S} = \rho/(2\omega)\text{Im}(\mathbf{v}^* \times \mathbf{v})$, and with Eq. (17) it is explicitly

$$\mathbf{S} = -\frac{|p_0|^2}{\rho_0\omega^3}\kappa k_y e^{-2\kappa x}\mathbf{e}_z, \quad (18)$$

and the torque due to spinning $\mathbf{T} = \omega\,\text{Im}(\alpha_d^y)\mathbf{S}$ [38] is also explicitly

$$\mathbf{T} = -\frac{|p_0|^2}{\rho_0\omega^2}\kappa k_y e^{-2\kappa x}\text{Im}(\alpha_d^y)\mathbf{e}_z. \quad (19)$$

Similarly, the gradient and scattering forces are given by

$$\mathbf{F}^{\text{grad}} = \text{Re}(\alpha_m)\nabla W^p + \text{Re}(\alpha_d^y)\nabla W^{\mathbf{v}},$$

$$\mathbf{F}^{\text{scatt}} = 2\omega[\text{Im}(\alpha_m)\mathbf{P}^p + \text{Im}(\alpha_d^y)\mathbf{P}^{\mathbf{v}}], \quad (20)$$

where we make use of [39,46]

$$\mathbf{P}^p = \frac{1}{4\omega}\text{Im}(\beta_0 p^*\nabla p), \quad W^p = \frac{\beta_0}{4}|p|^2,$$

$$\mathbf{P}^{\mathbf{v}} = \frac{1}{4\omega}\text{Im}(\rho_0[\mathbf{v}^* \cdot \nabla]\mathbf{v}), \quad W^{\mathbf{v}} = \frac{\rho_0}{4}|\mathbf{v}|^2. \quad (21)$$

Now, by combining Eqs. (15) and (16) (for the quasistatic case), along with Eqs. (19) and (20), we have access to
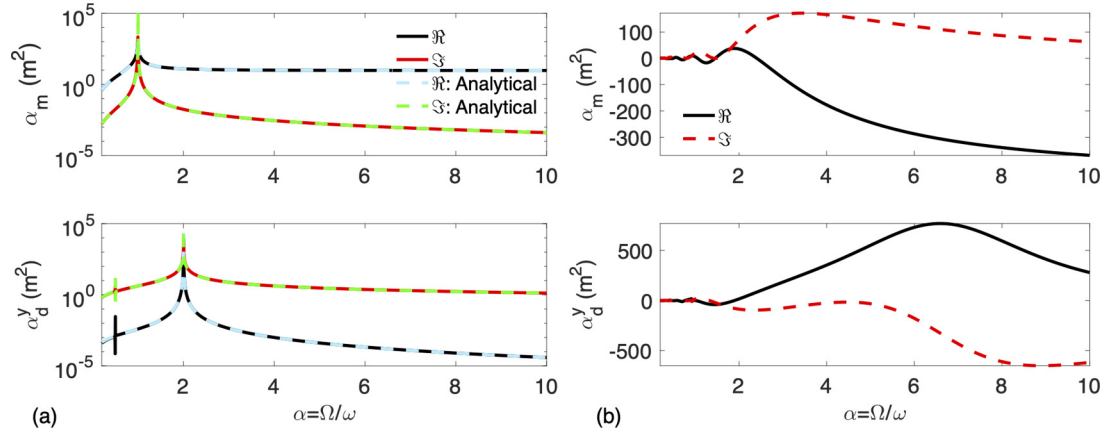
FIG. 2. (a) Absolute value of (top) the monopole polarizability α_m and (bottom) the dipole polarizability α_d^y, in logarithmic scale (i.e., $10\log_{10}$) vs $\alpha = \Omega/\omega$. The solid lines give the numerical results of both real and imaginary parts of (α_m, α_d^y) computed with Eq. (4) and Eqs. (13) and (14), while the dashed lines give analytical expressions obtained when $k_0 a \ll 1$, using Eqs. (15) and (16). The radius of the object is $a = 1$ m and $\Omega/(2\pi) = 10$ Hz. (b) Same as in (a) but for $a = 10$ m and $\Omega/(2\pi) = 100$ Hz. Please note that in (b) the scale is linear, unlike in (a), and that there is no analytical approximation, since $k_0 a \approx 1$.

the torque and force (gradient and scattering) experienced by the spinning object in the evanescent field. These results are depicted in Fig. 3(a), using the same parameters as those of Fig. 2(a). These quantities are normalized with $T_0 = -\pi \beta_0 |p_0|^2 a^2/(2k_0)$ and $F_0 = k_0 T_0$. Again, we find an excellent agreement between analytical and seminumerical results. Several resonances can be observed for T_z, F_y^{grad}, and F_x^{scatt}, stemming from the resonances of the polarizabilities. The important feature here is that an object of the same properties as the surrounding ($\rho = \rho_0$ and $\beta = \beta_0$) interacts with

inhomogeneous acoustic fields in an unexpected manner, as both torque and force can be experienced by this transparent object solely due to spinning.

The other scenario consists in using the exact value of ς_0 and $\varsigma_{\pm 1}$, by solving Eq. (4) and using them for the calculation of α_m and α_d^y, and subsequently the torque and force in a seminumerical manner [38]. Figure 3(b) gives the same responses in a more general case that cannot be treated analytically [similar as in Fig. 2(b)]. The torque and force are here of lower amplitude, due to the lack of resonances.
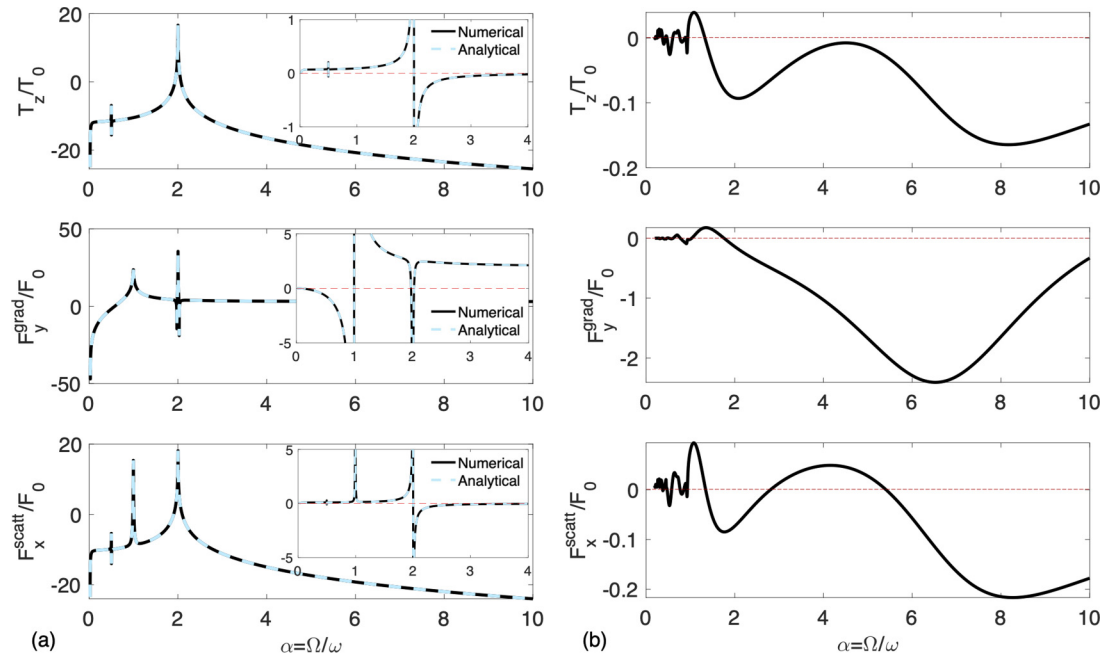
FIG. 3. (a) Logarithmic scale plot of the (top) normalized torque $10\log_{10}(T_z/T_0)$, (middle) normalized gradient force $10\log_{10}(F_y^{\text{grad}}/F_0)$, and (bottom) normalized scattering force $10\log_{10}(F_x^{\text{scatt}}/F_0)$, vs α. The solid (dashed) lines give the numerical (analytical) calculations, for the same object as of Fig. 2(a) and for $k_y/k_0 = 1.2$ and $\kappa/k_0 = 0.6633$. The insets in these plots show the linear scale plot of these parameters in a magnified view to showcase the regions where resonances occur and positive to negative values are obtained. (b) Same as in (a) but for the same object of Fig. 2(b). Please note that in (b) the scale is linear, unlike in (a). The red dashed lines denote zero values of the considered parameters.

The important feature of Fig. 3 is that both spin and force undergo positive/negative values for a specific spinning parameter α (highlighted by the red dashed lines). For instance, having negative force is paramount for obtaining a pulling effect. Recently, in Ref. [40] the condition for acoustic pulling was shown, i.e., the necessity to have either an active particle or a composite acoustic source, e.g., two incident waves making a finite angle. Yet, this study concerned only scatterers at rest. By allowing spinning, and even if $\rho = \rho_0$ and $\beta = \beta_0$, we can see that positive to negative force and spin can be obtained in a straightforward way, without the need for an active particle or complex incident wave.

To sum up, scattering from spinning acoustic objects was analytically and numerically characterized and shown to lead to an acoustic force and torque. Such objects, when present in evanescent acoustic fields, are shown to interact with the transverse spin even in the extreme case in which they possess a unit relative density and compressibility. Hence, the effects due to purely spinning can result in a surprising interaction of the rotating volume with the acoustic field in a way intrinsically different from regular static objects (i.e., $\rho/\rho_0 \neq 1$, $\beta/\beta_0 \neq 1$, and $\Omega = 0$). For instance, although the object is lossless, it experiences a net torque which is markedly different from objects at rest with a different impedance than the surrounding [38]. Similarly, the spinning domain feels both scattering and gradient forces. Several applications may result from this investigation, in which acoustic objects undergo rotation, e.g., for paving the way for fast acoustic communication devices [47] or Willis coupling [48].

[1] E. Graham and B. Graham, Effect of a shear layer on plane waves of sound in a fluid, J. Acoust. Soc. Am. **46**, 169 (1969).
[2] P. Peng, J. Mei, and Y. Wu, Lumped model for rotational modes in phononic crystals, Phys. Rev. B **86**, 134304 (2012).
[3] M. P. Lavery, F. C. Speirits, S. M. Barnett, and M. J. Padgett, Detection of a spinning object using light's orbital angular momentum, Science **341**, 537 (2013).
[4] S. Farhadi, Acoustic radiation of rotating and non-rotating finite length cylinders, J. Sound Vib. **428**, 59 (2018).
[5] D. Ramaccia, D. L. Sounas, A. Alù, A. Toscano, and F. Bilotti, Phase-induced frequency conversion and Doppler effect with time-modulated metasurfaces, IEEE Trans. Antennas Propag. **68**, 1607 (2020).
[6] Y. Mazor and B. Z. Steinberg, Rest Frame Interference in Rotating Structures and Metamaterials, Phys. Rev. Lett. **123**, 243204 (2019).
[7] B. Z. Steinberg, A. Shamir, and A. Boag, Two-dimensional Green's function theory for the electrodynamics of a rotating medium, Phys. Rev. E **74**, 016608 (2006).
[8] R. Novitski, B. Z. Steinberg, and J. Scheuer, Finite-difference time-domain study of modulated and disordered coupled resonator optical waveguide rotation sensors, Opt. Express **22**, 23153 (2014).
[9] Z. Liu, X. Zhang, Y. Mao, Y. Zhu, Z. Yang, C. T. Chan, and P. Sheng, Locally resonant sonic materials, Science **289**, 1734 (2000).
[10] P. A. Deymier, *Acoustic Metamaterials and Phononic Crystals*, Springer Series in Solid-State Sciences Vol. 173 (Springer, Berlin, 2013).
[11] R. V. Craster and S. Guenneau, *Acoustic Metamaterials: Negative Refraction, Imaging, Lensing and Cloaking*, Springer Series in Materials Science Vol. 166 (Springer, Berlin, 2012).
[12] Z. Liu, C. T. Chan, and P. Sheng, Analytic model of phononic crystals with local resonances, Phys. Rev. B **71**, 014103 (2005).
[13] J. Li and C. T. Chan, Double-negative acoustic metamaterial, Phys. Rev. E **70**, 055602(R) (2004).

[14] L.-W. Cai and J. Sánchez-Dehesa, Acoustical scattering by radially stratified scatterers, J. Acoust. Soc. Am. **124**, 2715 (2008).
[15] M. Amin, A. Elayouch, M. Farhat, M. Addouche, A. Khelif, and H. Bağcı, Acoustically induced transparency using Fano resonant periodic arrays, J. Appl. Phys. **118**, 164901 (2015).
[16] S. A. Cummer, J. Christensen, and A. Alù, Controlling sound with acoustic metamaterials, Nat. Rev. Mater. **1**, 16001 (2016).
[17] L. Quan, Y. Ra'di, D. L. Sounas, and A. Alù, Maximum Willis Coupling in Acoustic Scatterers, Phys. Rev. Lett. **120**, 254301 (2018).
[18] M. Landi, J. Zhao, W. E. Prather, Y. Wu, and L. Zhang, Acoustic Purcell Effect for Enhanced Emission, Phys. Rev. Lett. **120**, 114301 (2018).
[19] Y. Wu, M. Yang, and P. Sheng, Perspective: Acoustic metamaterials in transition, J. Appl. Phys. **123**, 090901 (2018).
[20] B. Assouar, B. Liang, Y. Wu, Y. Li, J.-C. Cheng, and Y. Jing, Acoustic metasurfaces, Nat. Rev. Mater. **3**, 460 (2018).
[21] M. F. Maghrebi, R. L. Jaffe, and M. Kardar, Spontaneous Emission by Rotating Objects: A Scattering Approach, Phys. Rev. Lett. **108**, 230403 (2012).
[22] D. Zutter, Scattering by a rotating circular cylinder with finite conductivity, IEEE Trans. Antennas Propag. **31**, 166 (1983).
[23] P. Hillion, Scattering by a rotating circular conducting cylinder I, Rep. Math. Phys. **41**, 223 (1998).
[24] B. Z. Steinberg, Rotating photonic crystals: A medium for compact optical gyroscopes, Phys. Rev. E **71**, 056621 (2005).
[25] B. Z. Steinberg and A. Boag, Splitting of microcavity degenerate modes in rotating photonic crystals—the miniature optical gyroscopes, J. Opt. Soc. Am. B **24**, 142 (2007).
[26] P. M. Morse, and K. U. Ingard, *Theoretical Acoustics* (Princeton University Press, Princeton, NJ, 1968).
[27] D. Censor and J. Aboudi, Scattering of sound waves by rotating cylinders and spheres, J. Sound Vib. **19**, 437 (1971).
[28] M. Schoenberg and D. Censor, Elastic waves in rotating media, Q. Appl. Math. **31**, 115 (1973).

[29] D. Censor and M. Schoenberg, Two dimensional wave problems in rotating elastic media, Appl. Sci. Research **27**, 401 (1973).

[30] M. Farhat, S. Guenneau, A. Alù, and Y. Wu, Scattering cancellation technique for acoustic spinning objects, Phys. Rev. B **101**, 174111 (2020).

[31] M. Farhat, P.-Y. Chen, S. Guenneau, S. Enoch, and A. Alu, Frequency-selective surface acoustic invisibility for three-dimensional immersed objects, Phys. Rev. B **86**, 174303 (2012).

[32] G. Dupont, M. Farhat, A. Diatta, S. Guenneau, and S. Enoch, Numerical analysis of three-dimensional acoustic cloaks and carpets, Wave Motion **48**, 483 (2011).

[33] D. Zhao, Y.-T. Wang, K.-H. Fung, Z.-Q. Zhang, and C. T. Chan, Acoustic metamaterials with spinning components, Phys. Rev. B **101**, 054107 (2020).

[34] A. Anhäuser, R. Wunenburger, and E. Brasselet, Acoustic Rotational Manipulation Using Orbital Angular Momentum Transfer, Phys. Rev. Lett. **109**, 034301 (2012).

[35] L. Burns, K. Y. Bliokh, F. Nori, and J. Dressel, Acoustic versus electromagnetic field theory: scalar, vector, spinor representations and the emergence of acoustic spin, New J. Phys. **22**, 053050 (2020).

[36] K. Y. Bliokh and F. Nori, Klein-Gordon Representation of Acoustic Waves and Topological Origin of Surface Acoustic modes, Phys. Rev. Lett. **123**, 054301 (2019).

[37] K. Y. Bliokh and F. Nori, Transverse spin and surface waves in acoustic metamaterials, Phys. Rev. B **99**, 020301(R) (2019).

[38] I. D. Toftul, K. Y. Bliokh, M. I. Petrov, and F. Nori, Acoustic Radiation Force and Torque on Small Particles as Measures of the Canonical Momentum and Spin Densities, Phys. Rev. Lett. **123**, 183901 (2019).

[39] K. Y. Bliokh and F. Nori, Spin and orbital angular momenta of acoustic beams, Phys. Rev. B **99**, 174310 (2019).

[40] Y. Meng, X. Li, Z. Liang, J. Ng, and J. Li, Acoustic Pulling With a Single Incident Plane Wave, Phys. Rev. Appl. **14**, 014089 (2020).

[41] See Supplemental Material at http://link.aps.org/supplemental/10.1103/PhysRevB.104.L060104 for the derivation of the modified wave equation governing the acoustic motion in spinning media as well as the derivation of the Mie scattering, which includes Refs. [31,32].

[42] E. Landau, *Handbuch der Lehre von der Verteilung der Primzahlen*, Vol. 1 (Chelsea Publishing, New York, 1953).

[43] The monopole strength is proportional to the derivative of a surface with respect to time (as we are in 2D) which corresponds to the expansion and compression of a cylindrical object with time.

[44] The dipole strength is proportional to the derivative of a volume with respect to time (as we are in 2D) which corresponds to the linear oscillatory motion of the cylindrical particle, induced by the velocity field, as schematically shown in Fig. 1(b) and where the scale of displacement is exaggerated to demonstrate the effect.

[45] J. Jordaan, S. Punzet, A. Melnikov, A. Sanches, S. Oberst, S. Marburg, and D. A. Powell, Measuring monopole and dipole polarizability of acoustic meta-atoms, Appl. Phys. Lett. **113**, 224102 (2018).

[46] C. Tang and G. A. McMechan, The dynamically correct Poynting vector formulation for acoustic media with application in calculating multidirectional propagation vectors to produce angle gathers from reverse time migration, Geophysics **83**, S365 (2018).

[47] C. Shi, M. Dubois, Y. Wang, and X. Zhang, High-speed acoustic communication by multiplexing orbital angular momentum, Proc. Natl. Acad. Sci. USA **114**, 7250 (2017).

[48] H. Esfahlani, Y. Mazor, and A. Alù, Homogenization and design of acoustic Willis metasurfaces, Phys. Rev. B **103**, 054306 (2021).